Title	Transient formation of intermediate conformational states of amyloid-β peptide revealed by heteronuclear magnetic resonance spectroscopy.
Author(s)	Yamaguchi, Takahiro; Matsuzaki, Katsumi; Hoshino, Masaru
Citation	FEBS letters (2011), 585(7): 1097-1102
Issue Date	2011-04-06
URL	http://hdl.handle.net/2433/139746
Right	© 2011 Federation of European Biochemical Societies Published by Elsevier B.V.
Type	Journal Article
Textversion	author

Transient formation of intermediate conformational states of amyloid-β peptide revealed by heteronuclear magnetic resonance spectroscopy

Takahiro Yamaguchi, Katsumi Matsuzaki and Masaru Hoshino*

Graduate School of Pharmaceutical Sciences, Kyoto University, 46-29 Yoshida-Shimoadachi, Sakyo-ku, Kyoto 606-8501, Japan

*Corresponding author.

Masaru Hoshino

Graduate School of Pharmaceutical Sciences, Kyoto University

46-29 Yoshida-Shimoadachi, Sakyo-ku, Kyoto 606-8501, Japan

Phone: +81-75-753-4531

Fax: +81-75-753-4529

E-mail: hoshi@pharm.kyoto-u.ac.jp

Abstract

A detailed analysis of the NMR spectra of amyloid-β (Aβ) peptide revealed a decrease in signal intensity at higher temperature, due to a reversible conformational change of the molecule. Although peak intensity did not depend on peptide concentrations, the intensity in the region from D23 to A30 depended significantly on temperature. During the early stages of Aβ aggregation, each molecule might adopt transiently a turn conformation at around D23–A30, which converts mutually with a random coil. Stabilization of a turn by further conformational change and/or molecular association would lead to the formation of a "nucleus" for amyloid fibrils.

Keywords: NMR, amyloid fibril formation, conformational change, chemical exchange

Abbreviations: AD, Alzheimer's disease; Aβ, amyloid-β peptide; NMR, nuclear magnetic resonance; HSQC, heteronuclear single-quantum coherence; TOCSY, total correlation spectroscopy; WATERGATE, WATER supression by GrAdient Tailored Excitation

1. Introduction

The conversion of a soluble, nontoxic molecule to a β-sheet-rich structure is a hallmark of amyloidoses including Alzheimer's disease (AD) [1-3]. The major component of amyloid fibrils deposited in AD brains is amyloid β-peptide (Aβ), which is generated from the proteolytic cleavage of amyloid precursor protein by β- and γ-secretases. The molecular structure of Aβ amyloid fibrils has been revealed in detail by recent advances in solid-state NMR spectroscopy. Aβ fibrils are suggested to form in-register parallel β-sheets with each molecule assuming a strand-turn-strand conformation, the β-strands of V12–V24 and A30–V40 connected by a turn at G25–G29 [4-6].

Although the aggregation of Aβ is considered a key step in the onset and development of AD, the molecular species exerting the neurotoxicity remain controversial. To date, a variety of Aβ oligomers with different degrees of neurotoxicity and structural properties have been identified such as Aβ dimers, Aβ-derived diffusible ligands (ADDLs), globulomers, Aβ*56, amylospheroids and spherical intermediate (I_{β}) [7, 8]. In addition, Aβ forms fibrils differing in morphology and neurotoxicity depending on the incubation conditions [5, 9]. Since Aβ forms diverse aggregates, it is important to elucidate the mechanism of aggregation, especially in the early stages.

The most convincing model for the development of amyloid fibrils is the nucleation-dependent polymerization model [10, 11]. According to this model, the fibrillation process is separated into a nucleation phase and an elongation phase. Monomeric protein is thought to self-associate and form a nucleus through conformational change. The nucleation process is thermodynamically unfavorable,

resulting in a long lag-phase in the kinetics of amyloid fibril formation. Once the nucleus is formed, however, the binding of the monomer proceeds rapidly. Although the nucleation is a critical step, its precise mechanism is unknown because of its transient nature.

Nuclear magnetic resonance (NMR) spectroscopy is one of the most powerful techniques for analyzing the structure, dynamics and function of proteins in solution. In addition, it provides a unique means of detecting "minor" conformations that exist only transiently [12, 13]. On analyzing ^{1}H-^{15}N and ^{1}H-^{13}C HSQC spectra of Aβ-(1–40) in detail, we found that the signal intensity decreased significantly at higher temperature. We show that the decrease in peak height is due to a reversible conformational exchange of the Aβ molecule. Notably, the region from D23 to A30 exhibited a significant decrease in peak intensity with increasing temperature. The decrease did not depend on peptide concentrations, suggesting an intramolecular conformational exchange. During the early stages of Aβ aggregation, each molecule probably adopts a transiently folded structure with a turn at around D23–A30, which is converted mutually with a random coil conformation. Stabilization of the transient structure by further conformational change and/or molecular association would lead to the formation of a "nucleus" for amyloid fibrils.

2. Materials and Methods

2.1. Materials

^{15}N-Ammonium chloride, U-$^{13}C_6$-glucose, deuterium oxide and sodium 2,2-dimethyl-2-silapentane-5-sulfonate (DSS) were purchased from SI Science Co. Ltd. Other reagents were purchased from Nacalai Tesque.

2.2. Protein preparation

Expression and purification of the Aβ-(1–40) peptide were performed as described previously [14]. For the preparation of uniformly ^{15}N-, or ^{13}C,^{15}N-labeled peptides, bacterial cells were grown in M9 minimal medium supplied with 0.5 g/L $^{15}NH_4Cl$, or 2 g/L ^{13}C-glucose and 0.5 g/L $^{15}NH_4Cl$, respectively.

2.3. NMR measurements

NMR spectra were measured on a Bruker DMX600 spectrometer equipped with a triple-axis gradient TXI probe. ^{15}N-labeled or ^{13}C,^{15}N-labeled Aβ-(1–40) was dissolved in 50 mM sodium phosphate (pH 6.5), 100 mM NaCl, and 10% or 100% D_2O. The peptide concentration was 20–75 μM and 150 μM for 2D and 3D measurements, respectively. Backbone and side-chain resonance assignments were performed at 4 °C by analyzing 3D HNCACB, HN(COCA)HA, and HCCH-TOCSY spectra. The assignments at other temperatures were obtained by following the change in signal shifts upon gradually increasing the temperature. The chemical shift value was referenced with sodium 2,2-dimethyl-2-silapentane-5-sulfonate (DSS). The spectra were processed with nmrPipe and analyzed with nmrDraw and PIPP [15, 16].

3. Results

3.1. Temperature-dependent signal attenuation in ^{1}H-^{15}N HSQC spectra

We first measured ^{1}H-^{15}N HSQC spectra of Aβ-(1–40) at pH 6.5 and various temperatures (Fig. 1). The cross peaks of Aβ-(1–40) were poorly dispersed, indicating that neither a well-defined secondary nor a rigid tertiary structure was formed under the

conditions examined. By conducting a series of triple resonance experiments as well as analyzing the HCCH-TOCSY spectrum, all the backbone and most of the side chain resonances could be unambiguously assigned (supplementary table S1). At 4 °C, all the backbone amide cross-peaks except for the N-terminal Asp were observed. On increasing the temperature, whereas the chemical shift value of each resonance peak did not change significantly, the intensity (peak height) decreased. This was, however, unexpected. The peak hight of Lorentzian line shape is inversely proportional to the transverse rate constant, R_2, which is approximately proportional to the overall rotational correlation time, τ_C, of the molecule. As a protein molecule tumbles faster (smaller τ_C) at higher temperature, the NMR signals become sharper and their intensity should increase with temperature. On the contrary, we found that the signal intensity of Aβ-(1–40) decreased at higher temperature. Considering that Aβ-(1–40) has a strong tendency to form amyloid fibrils, one of the simplest explanations for this phenomenon would be irreversible aggregation during measurement at increasing temperature. However, the ^{1}H-^{15}N HSQC spectrum at 4 °C recorded after the increase in temperature showed the same intensity as that recorded before the temperature rise, demonstrating that the above observations were not due to the irreversible aggregation of Aβ (Fig. 1D).

3.2. Elimination of the exchange with water: ^{1}H-^{13}C HSQC spectra

Another possible explanation for this signal reduction at higher temperature is exchange with water molecules. The signal intensity in ^{1}H-^{15}N HSQC spectra depends significantly on the rate constant of exchange between labile amide protons and solvent water. To minimize the effect of exchange with solvent water, we utilized the binominal (3-9-19) WATERGATE pulse train as well as water flip-back scheme to suppress water

signals when recording ^{1}H-^{15}N HSQC spectra [17, 18]. Nevertheless, it is still possible that increased exchange with solvent water at higher temperature attenuated the cross-peak intensity in ^{1}H-^{15}N HSQC spectra. We therefore examined the temperature dependency of signal intensity in the ^{1}H-^{13}C HSQC spectra, in which no significant effect of exchange with solvent water was expected. Figure 2 shows the ^{1}H-^{13}C HSQC spectra of Aβ-(1–40) recorded under the same conditions as those of Fig. 1 except that the solution contained 100% D_2O instead of 90% H_2O/10 % D_2O. Although several side-chain resonances could not be assigned unambiguously due to significant overlapping (supplementary Table S1), the results clearly demonstrated again that the signal intensity was decreased at higher temperature. Notably, almost all the H_α-C_α cross peaks were missing at 37 °C (supplementary Fig. S1). These results emphasize that another mechanism is required to explain the apparently anomalous temperature dependency of the peak intensity in both the ^{1}H-^{15}N and ^{1}H-^{13}C HSQC spectra. We consider the most probable mechanism for this phenomenon to be the chemical exchange between different nuclear environments caused by the temporary formation of another conformational state in the Aβ-(1–40) molecules.

3.3. Backbone versus side chain dynamics

The dependency of peak intensity on temperature in the ^{1}H-^{13}C and ^{1}H-^{15}N HSQC spectra of Aβ-(1–40) was analyzed further in detail. Figure 3 shows the relative peak intensity of several representative residues as a function of temperature, taken from Figs. 1, 2 and S1. It was revealed that the cross peak intensity of two pairs of backbone atoms, H_α-C_α and H_N-N, depended significantly on the temperature. The two cross-peaks exhibited similar temperature dependency, and the relative intensity for most of the

residues at 37 °C was found to decrease to ~20% of that at 4 °C. In contrast, the cross-peak intensity of side chain atoms was relatively tolerant of the temperature shift, and most of the H_β-C_β and H_γ-C_γ cross peaks decreased to only 60–80%.

3.4. Considerable decrease in intensity around the region of D23–A30

To elucidate whether the temperature dependency of peak intensity is site specific, the relative intensity of amide protons was plotted against residue number (Fig. 4). Several residues, such as A2, H6, H13, H14 and Q15, were excluded from the analysis because of a low signal intensity even at 4 °C. Two additional residues, V24 and I31, were also eliminated because these peaks overlapped at temperatures higher than 13 °C. It should be noted, however, that the intensity of the overlapping cross peak derived from V24 and I31 decreased ~50% at 17 °C, indicating that these two residues also considerably depend on temperature. The overall distribution of relative peak intensity along the sequence was not uniform but showed a positional dependency. Notably, the consecutive region around D23–A30 was most sensitive to temperature, with relative intensity at 17 °C only 40–60%. On the other hand, other residues were insensitive to temperature change except S8, G9, G37 and G38, which decreased significantly.

3.5. Intramolecular conformational exchange revealed by peptide concentration dependency

The decrease in peak intensity is considered to be the result of the shift from the slow to intermediate exchange regime upon the increase in temperature (see discussion). We speculated that similar results could be obtained by increasing the peptide concentration if the observed chemical exchange resulted from association/dissociation

between monomeric peptides. However, signal intensity would not depend on the peptide concentration if the chemical exchange occurred within a molecule. To elucidate whether the chemical exchange results from intra- or intermolecular conformational change of the Aβ peptide, ^{1}H-^{15}N HSQC spectra of ^{15}N-labeled Aβ-(1–40) were measured in the absence or presence of an excess amount of unlabeled Aβ at 4 °C. Surprisingly, the excess amount of unlabeled Aβ peptide did not affect the peak intensity in the ^{1}H-^{15}N HSQC spectrum (Figure 5), indicating that the observed chemical exchange is not due to the intermolecular association/dissociation, and that each molecule of Aβ-(1–40) is in dynamic equilibrium between several different conformational states.

4. Discussion

The linewidth of solution NMR signals depends on the overall rotational correlation time, τ_C, as well as the internal mobility of the protein molecule. Both dynamical motions become larger at higher temperature, and therefore signal intensity is also expected to increase with temperature. However, we found that the signal intensity of Aβ-(1–40) in both the ^{1}H-^{15}N and ^{1}H-^{13}C HSQC spectra decreased with increasing temperature. Moreover, signals that disappeared at higher temperature were recovered by lowering the temperature, indicating that the decrease in peak intensity was not due to irreversible aggregation. Instead, the decrease in signal intensity at higher temperature would be caused by chemical exchange between several different magnetic environments experienced by each nuclear spin.

The chemical exchange in NMR measurements is usually classified as “slow”,

"intermediate", or "fast", depending on the relative value of the exchange rate constant, k_{ex}, and chemical shift difference between the two states, $\Delta\omega = |\Omega_A - \Omega_B|$ [19, 20] (Supplementary Fig. S2). If the exchange rate is in the order of the chemical shift difference between the two sites, $k_{ex} \sim \Delta\omega$, both resonance lines will apparently "disappear" because of severe line broadening. This is known as chemical exchange line broadening.

In the present study, while the peak intensity in the ^{1}H-^{15}N and ^{1}H-^{13}C HSQC spectra was found to decrease dramatically upon raising the temperature, neither chemical shift change nor the appearance of new NMR signals occurred. Most chemical reactions are generally enhanced at higher temperature, and therefore, an increase in temperature should cause a shift in conditions from (i) "slow" to "intermediate" or (ii) "intermediate" to "fast" exchange. However, the latter would result in sharper, more intense resonance signals at higher temperature, which is opposite to the present results. On the other hand, in situation (i), two resolved peaks will appear under conditions of "slow" exchange. Nevertheless, we observed only a single peak for each pair of ^{1}H-^{15}N or ^{1}H-^{13}C even under low temperature conditions. This indicates that the equilibrium is extremely biased to either side of the reaction, in which the population of "minor" conformations is much lower than the detection limit. It should be noted here that the apparent decrease in intensity at higher temperature can be caused by an increase in the rate of interconversion, and is not necessarily involved in the decrease in the population (Supplementary Fig. S2).

While the cross peak intensity of backbone signals (H_N-N and H_α-C_α) showed a similar temperature dependency, that of side-chain signals was less significant (Fig. 3). This indicates that the conformational exchange affected the backbone signals more

drastically than the signals from side-chain atoms. One of the possible explanations for this difference is that the conformational exchange involves backbone atoms, e.g., the transient formation of hydrogen bonds between H_N and carbonyl oxygen.

Another important finding of the present study was that the effect of temperature shift differed considerably among residues (Fig. 4). That is, D23–A30 exhibited larger decreases in peak intensity than other regions, indicating that the residues in this region experience two or more different magnetic environments. As shown in supplementary Fig. S2, the degree of chemical exchange line broadening depends significantly on the amplitude of chemical shift difference between two states ($\Delta\omega = |\Delta\Omega_A - \Delta\Omega_B|$). Although we do not know the exact value of $\Delta\omega$ for each residue because the population of the "minor" conformation is under the detection limit, the residues in the region of D23–A30 may have larger $\Delta\omega$ values than other residues. This means that a nuclear spin in this region experiences a drastic change in the chemical environment when the molecule adopts the "minor" conformation.

In contrast to the effect of an increase in temperature, signal intensity was not affected by the total peptide concentration, as revealed by comparing the ^{1}H-^{15}N HSQC spectra of ^{15}N-labeled Aβ-(1–40) measured in the absence and presence of an excess amount of unlabeled peptide (Fig. 5). Therefore, the chemical exchange would be caused by the intra-molecular interaction. Considering all of these observations, we presume that an Aβ-(1–40) molecule in solution is in dynamic equilibrium between a random coil conformation and a folded structure with a turn at around D23–A30 (Fig. 6). This partially folded structure is probably stabilized by the temporary formation of intramolecular hydrogen bonds between backbone atoms.

A similar turn conformation has been characterized in a variety of molecular

species of Aβ peptides. The formation of a turn at G25–G29 is supposed in the amyloid fibril structure modeled by solid-state NMR [4, 6]. A β-hairpin conformation with a turn at D23–A30 was found in a monomeric Aβ bound to affibody $Z_{Aβ3}$ [21]. Furthermore, the stabilization of a similar β-hairpin conformation via disulfide bridge resulted in a formation of toxic oligomeric species [22]. Intramolecular β-hairpin with a turn at D23–K28 is also suggested by the NMR analysis of soluble oligomer [23]. In addition, Lazo et al. reported that the A21–A30 region of Aβ-(1–40) was highly resistant to protease cleavage and that the V24–K28 region of the decapeptide Aβ-(21–30) adopted a turn conformation exemplified by solution-state NMR [24]. Furthermore, several molecular dynamics simulations also support the formation of a hairpin-like structure in this region [25, 26].

We should emphasize that the turn conformation suggested in the present study is maintained only transiently, as indicated by the low population below the detection limit. Such a transient, short-lived conformation might represent the key intermediate structure that is obligatory for the growth into amyloid fibrils. Sciarretta et al. have shown that Aβ-(1–40) with a lactam bridge between D23 and K28 forms amyloid fibrils much more rapidly than wild-type peptide with no lag phase in fibril formation [27]. They concluded that the lactam bridge confers a bend-like structure, which bypasses an unfavorable folding step in fibrillogenesis. Aβ-(1–40) can adopt a turn structure, but this conformation is thermodynamically unfavorable. The Aβ molecule in solution probably adopts a transiently folded structure with a turn at around D23–A30, which is reversibly interconverting with a random coil conformation. Such a transient formation of the intermediate conformation might occur repeatedly during the early stages of Aβ

aggregation.

Recently, Fawzi et al. [28] analyzed the chemical exchange between the monomer and NMR-invisible large oligomer, under conditions of a stable pseudo-equilibrium between them. While they found a significant contribution of the chemical exchange enhancement of the $^{1}H_{N}$ and ^{15}N relaxation rate constant at a higher concentration range (150–300 μM), no evidence of such oligomeric states was observed under a similar peptide concentration (60 μM) to the present study (50–75 μM). Nevertheless, detailed analysis of the results of saturation transfer experiments suggested that cross-relaxation among protons within the monomer occurs even under oligomer-free conditions with a low peptide concentration. These results were consistent with the present study. Whereas the intermolecular chemical exchange between the monomer and oligomer occurs efficiently at higher peptide concentrations, a hairpin conformation would also be formed transiently in each molecule.

According to these observations, we found recently that disulfide-linked dimeric Aβ peptides aggregated very rapidly to form kinetically trapped protofibril-like oligomers [14]. The results indicated the importance of the conformational flexibility of the Aβ molecule and a balance in the association and dissociation rate for the formation of rigid amyloid fibrils. A dynamic rearrangement in each molecule as evidenced by the present study as well as association/dissociation between molecules must occur repeatedly during the lag-period of amyloid fibril formation. Stabilization of this only transiently formed turn conformation by the association of several molecules probably leads to the formation of the “nucleus” or the “seed” for the amyloid fibrils. Reagents destabilizing this turn conformation would be promising drugs for inhibiting Aβ aggregation and aggregate-induced neurotoxicity.

Acknowledgements

This work was supported by the Sankyo Foundation of Life Science, and by the Research Funding for Longevity Sciences (22-14) from National Center for Geriatrics and Gerontology (NCGG), Japan.

Appendix A. Supplementary data

Supplementary data associated with this article (Figures S1, S2 and Table S1) can be found in the online version.

References

1. Hardy, J., and Selkoe, D. J. (2002) The amyloid hypothesis of Alzheimer's disease: progress and problems on the road to therapeutics, *Science 297*, 353-356.
2. Harper, J. D., and Lansbury, P. T., Jr. (1997) Models of amyloid seeding in Alzheimer's disease and scrapie: mechanistic truths and physiological consequences of the time-dependent solubility of amyloid proteins, *Annu Rev Biochem 66*, 385-407.
3. Selkoe, D. J. (1994) Cell biology of the amyloid beta-protein precursor and the mechanism of Alzheimer's disease, *Annu Rev Cell Biol 10*, 373-403.
4. Petkova, A. T., Ishii, Y., Balbach, J. J., Antzutkin, O. N., Leapman, R. D., Delaglio, F., and Tycko, R. (2002) A structural model for Alzheimer's beta -amyloid fibrils based on experimental constraints from solid state NMR, *Proc Natl Acad Sci U S A 99*, 16742-16747.
5. Petkova, A. T., Leapman, R. D., Guo, Z., Yau, W. M., Mattson, M. P., and Tycko, R. (2005) Self-propagating, molecular-level polymorphism in Alzheimer's beta-amyloid

fibrils, *Science 307*, 262-265.

6. Petkova, A. T., Yau, W. M., and Tycko, R. (2006) Experimental constraints on quaternary structure in Alzheimer's beta-amyloid fibrils, *Biochemistry 45*, 498-512.
7. Glabe, C. G. (2008) Structural classification of toxic amyloid oligomers, *J. Biol. Chem. 283*, 29639-29643.
8. Roychaudhuri, R., Yang, M., Hoshi, M. M., and Teplow, D. B. (2009) Amyloid β-protein assembly and Alzheimer disease, *J. Biol. Chem. 284*, 4749-4753.
9. Okada, T., Ikeda, K., Wakabayashi, M., Ogawa, M., and Matsuzaki, K. (2008) Formation of toxic Aβ(1-40) fibrils on GM1 ganglioside-containing membranes mimicking lipid rafts: polymorphisms in Aβ(1-40) fibrils, *J Mol Biol 382*, 1066-1074.
10. Jarrett, J. T., and Lansbury, P. T., Jr. (1993) Seeding "one-dimensional crystallization" of amyloid: a pathogenic mechanism in Alzheimer's disease and scrapie?, *Cell 73*, 1055-1058.
11. Naiki, H., and Gejyo, F. (1999) Kinetic analysis of amyloid fibril formation, *Methods Enzymol 309*, 305-318.
12. Eisenmesser, E. Z., Millet, O., Labeikovsky, W., Korzhnev, D. M., Wolf-Watz, M., Bosco, D. A., Skalicky, J. J., Kay, L. E., and Kern, D. (2005) Intrinsic dynamics of an enzyme underlies catalysis, *Nature 438*, 117-121.
13. Korzhnev, D. M., Salvatella, X., Vendruscolo, M., Di Nardo, A. A., Davidson, A. R., Dobson, C. M., and Kay, L. E. (2004) Low-populated folding intermediates of Fyn SH3 characterized by relaxation dispersion NMR, *Nature 430*, 586-590.
14. Yamaguchi, T., Yagi, H., Goto, Y., Matsuzaki, K., and Hoshino, M. (2010) A disulfide-linked amyloid-beta peptide dimer forms a protofibril-like oligomer

through a distinct pathway from amyloid fibril formation, *Biochemistry 49*, 7100-7107.

15. Delaglio, F., Grzesiek, S., Vuister, G. W., Zhu, G., Pfeifer, J., and Bax, A. (1995) NMRPipe: a multidimensional spectral processing system based on UNIX pipes, *J Biomol NMR 6*, 277-293.
16. Garrett, D. S., Powers, R., Gronenborn, A. M. and Clore, G. M. (1991) A common sense approach to peak picking in two, three and four-dimensional spectra using automatic computer analysis of contour diagrams. *J Magn. Reson.* **95**, 214–220.
17. Grzesiek, S. & Bax, A. (1993) The importance of not saturating H_2O in protein NMR. Application to sensitivity enhancement and NOE measurements. *J. Am. Chem. Soc.* 115, 12593-12594.
18. Sklenár, V., Piotto, M., Leppik, R., Saudek, V. (1993) Gradient-tailored water suppression for ^{1}H-^{15}N HSQC experiments optimized to retain full sensitivity. *J. Magn. Reson. A* 102, 241-245.
19. Cavanagh, J., Fairbrother, W. J., Palmer, III, A. G., Rance, M. & Skelton, N. J. "Protein NMR spectroscopy, 2nd Ed." pp. 333–404. Academic Press, Oxford, 2007.
20. Palmer, A. G., 3rd, Kroenke, C. D., and Loria, J. P. (2001) Nuclear magnetic resonance methods for quantifying microsecond-to-millisecond motions in biological macromolecules, *Methods Enzymol 339*, 204-238.
21. Hoyer, W., Grönwall, C., Jonsson, A., Ståhl, S., and Härd, T. (2008) Stabilization of a β-hairpin in monomeric Altzheimer's amyloid-β peptide inhibits amyloid formation. *Proc. Natl. Acad. Sci. USA*, **105**, 5099–5104.
22. Sandberg, A., Luheshi, L. M., Söllvander, S., de Barros, T. P., Macao, B., Knowles, T. P. J., Biverstål, H., Lendel, C., Ekholm-Petterson, F., Dubnovitsky, A., Lannfelt,

L., Dobson, C. M., and Härd, T. (2010) Stabilization of neurotoxic Alzheimer amyloid-β oligomers by protein engineering. *Proc. Natl. Acad. Sci. USA*, **107**, 15595–15600.

23. Yu, L., Edalji, R., Harlan, J. E., Holzman, T. F., Lopez, A. P., Labkovsky, B., Hillen, H., Barghorn, S., Ebert, U., Richardson, P. L., Miesbauer, L., Solomon, L., Bartley, D., Walter, K., Johnson, R. W., Hajduk, P. J., and Olejniczak, E. T. (2009) Structural characterization of a soluble amyloid β-peptide oligomer. *Biochemistry*, **48**, 1870–1877.

24. Lazo, N. D., Grant, M. A., Condron, M. C., Rigby, A. C., and Teplow, D. B. (2005) On the nucleation of amyloid beta-protein monomer folding, *Protein Sci 14*, 1581-1596.

25. Borreguero, J. M., Urbanc, B., Lazo, N. D., Buldyrev, S. V., Teplow, D. B, and Stanley, H. E. (2005) Folding events in the 21–30 region of amyloid β-protein (Aβ) studied *in silico*, *Proc. Natl. Acad. Sci. USA, 102*, 6015–6020.

26. Han, W., Wu, Y.-D. (2005) A strand-loop-strand structure is a possible intermediate in fibril elongation: Long time simulations of amyloid-β peptide (10–35), *J. Am. Chem. Soc. 127*, 15408–15416.

27. Sciarretta, K. L., Gordon, D. J., Petkova, A. T., Tycko, R., and Meredith, S. C. (2005) Abeta40-Lactam(D23/K28) models a conformation highly favorable for nucleation of amyloid, *Biochemistry 44*, 6003-6014.

28. Fawzi, N. L., Ying, J., Torchia, D. A., and Clore, G. M. (2010) Kinetics of amyloid beta monomer-to-oligomer exchange by NMR relaxation, *J Am Chem Soc 132*, 9948-9951.

Figure legends

Figure 1. Reversible decrease in the signal intensity of the ^{1}H-^{15}N HSQC spectrum with increasing temperature. Fifty micromolar of ^{15}N-labeled Aβ-(1–40) was dissolved in 50 mM sodium phosphate (pH 6.5), 100 mM NaCl and 10% D_2O, and ^{1}H-^{15}N HSQC spectra were measured in order at 4 °C (A), 25 °C (B), 37 °C (C) and 4 °C (D). The peak of Ala2, which should appear at 8.29 ($^{1}H_N$) and 123.8 (^{15}N) ppm in (a), is too weak to be visible at this threshold level. Suppression of the solvent water signal was performed by the binominal (3-9-19) WATERGATE pulse train with water flip-back scheme to minimize the effect of exchange when recording the spectra [17, 18].

Figure 2. Reversible decrease in the signal intensity of the ^{1}H-^{13}C HSQC spectrum with increasing temperature. Seventy five micromolar of ^{15}N,^{13}C-labeld Aβ-(1–40) was dissolved in 50 mM sodium phosphate (pH 6.5), 100 mM NaCl and 100% D_2O, and ^{1}H-^{13}C HSQC spectra were measured in order at 4 °C (A), 25 °C (B), 37 °C (C) and 4 °C (D). The region typical for H_α-C_α cross peaks are indicated by dotted square.

Figure 3. Temperature-dependent decrease in peak intensity of ^{1}H-^{15}N and ^{1}H-^{13}C HSQC spectra. The intensity relative to that at 4 °C is plotted against temperature. Cross peaks of $^{1}H_N$-^{15}N, $^{1}H_\alpha$-$^{13}C_\alpha$ and the other signals from the side chain ($^{1}H_\beta$-$^{13}C_\beta$, $^{1}H_\gamma$-$^{13}C_\gamma$, $^{1}H_\delta$-$^{13}C_\delta$) are shown by blue, red and black lines, respectively. Several cross peaks derived from the same amino acid type, such as $^{1}H_\alpha$-$^{13}C_\alpha$ of A2 and A30, overlapped with each other, and are drawn with the same line.

Figure 4. Cross peak intensities of ^{1}H-^{15}N HSQC spectra measured at 17 °C (red) and 25 °C (blue) plotted against residue number. The intensity relative to that at 4 °C is shown. Several cross peaks which were quite weak, such as A2, H6, H13, H14, and Q15, were excluded from the analysis, and are indicated by closed diamonds. Two overlapping peaks, V24 and I31, are indicated by closed squares. The residues whose intensity decreased dramatically (< 0.6 at 17 °C) upon the temperature increase are indicated in orange bands.

Figure 5. ^{1}H-^{15}N HSQC spectra of ^{15}N-labeled Aβ-(1–40) peptide in the absence (red) and presence (blue) of an excess amount of non-labeled peptide. Sample concentrations were 20 μM ^{15}N-Aβ, or 20 μM ^{15}N-Aβ and 200 μM ^{14}N-Aβ. Other conditions were the same as those for Fig. 1A (4 °C). Several residues close to three histidine residues (H6, H13 and H14) were slightly shifted, probably due to the unexpected subtle change in pH around 6.5.

Figure 6. Schematic drawing of chemical exchange between the random coil structure and a minor conformation suggested by this study. A hairpin conformation with a turn around D23–A30, which is transiently stabilized by backbone hydrogen bonds, is indicated.

Figure(s)

Click here to download high resolution image

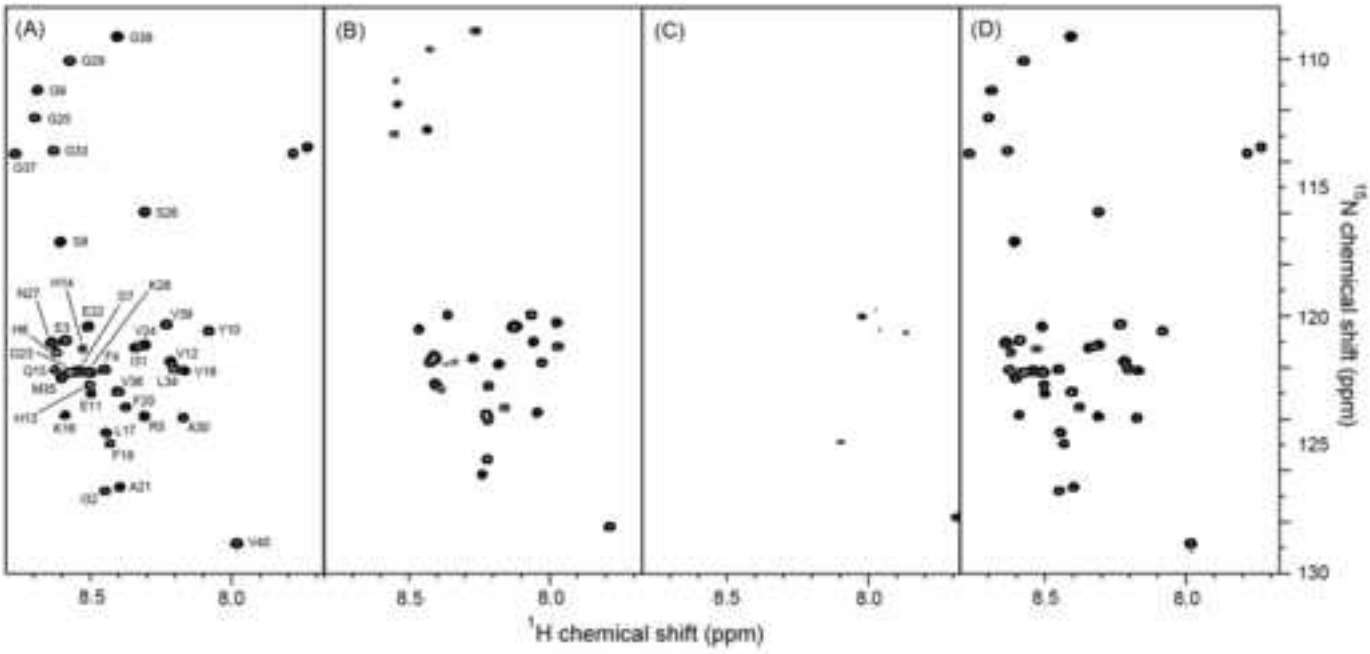

Yamaguchi et al., Fig. 1

Figure(s)

Click here to download high resolution image

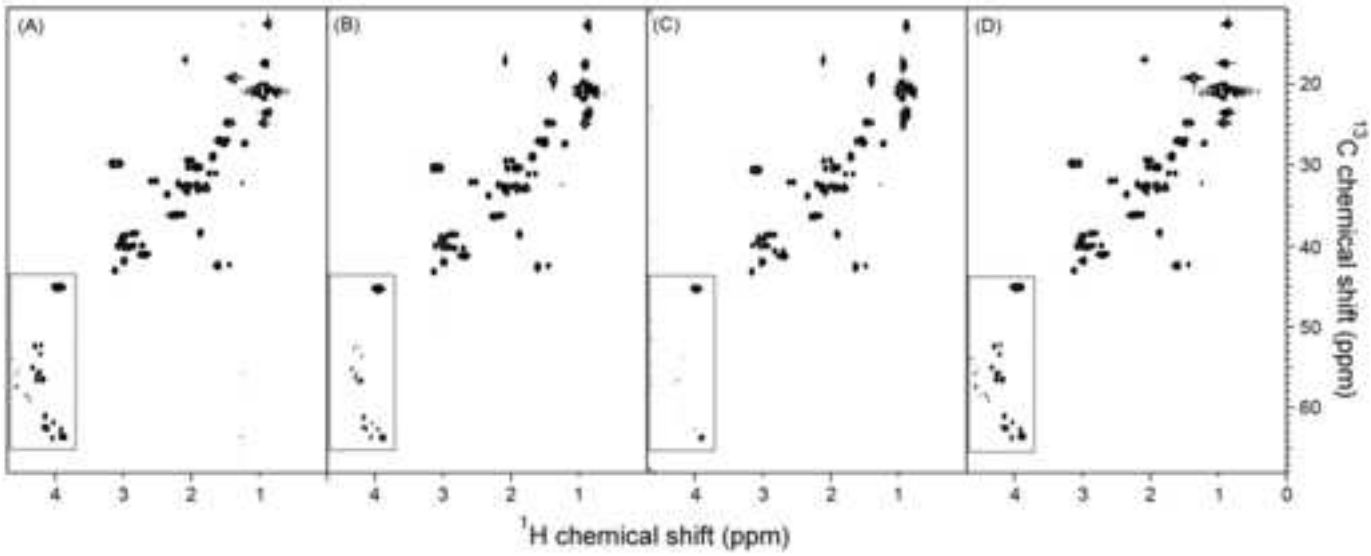

Yamaguchi et al., Fig. 2

Figure(s)

Click here to download high resolution image

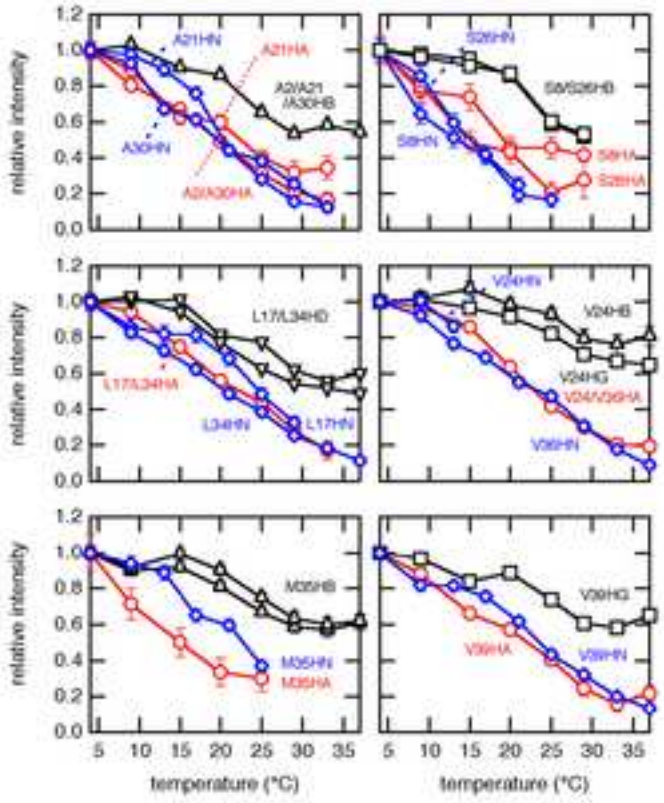

Yamaguchi et al., Fig. 3

Figure(s)

Click here to download high resolution image

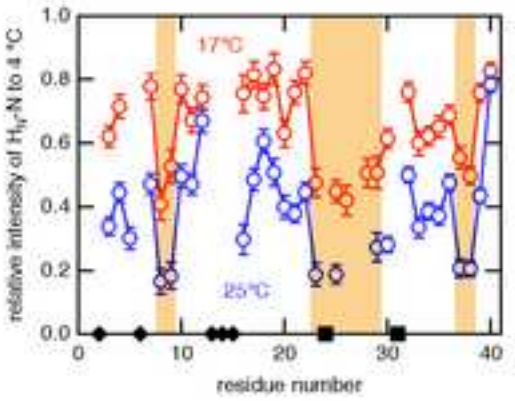

Yamaguchi et al., Fig. 4

Figure(s)

Click here to download high resolution image

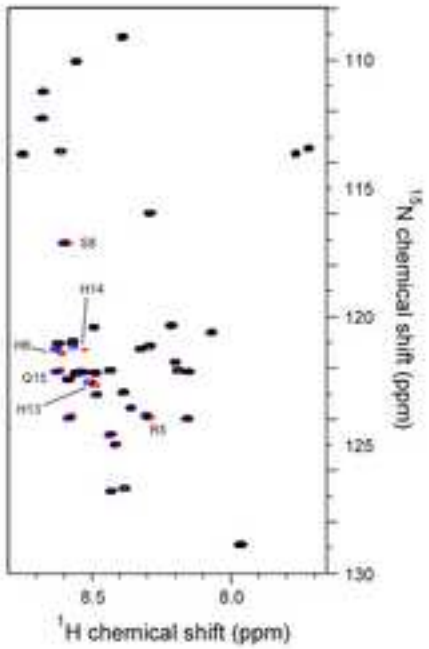

Yamaguchi et al., Fig. 5

Figure(s)

Click here to download high resolution image

Yamaguchi et al., Fig. 6